

Video Article

Fabrication and Testing of Microfluidic Optomechanical Oscillators

Kewen Han¹, Kyu Hyun Kim², Junhwan Kim¹, Wonsuk Lee^{2,3}, Jing Liu³, Xudong Fan³, Tal Carmon², Gaurav Bahl¹

¹Mechanical Science and Engineering, University of Illinois at Urbana-Champaign

²Electrical Engineering and Computer Science, University of Michigan

³Biomedical Engineering, University of Michigan

Correspondence to: Gaurav Bahl at bahl@illinois.edu

URL: <https://www.jove.com/video/51497>

DOI: [doi:10.3791/51497](https://doi.org/10.3791/51497)

Keywords: Physics, Issue 87, Optomechanics, Radiation pressure, Stimulated Brillouin scattering (SBS), Whispering gallery resonators (WGR), Oscillators, Microfluidics, Nonlinear Optics

Date Published: 5/29/2014

Citation: Han, K., Kim, K.H., Kim, J., Lee, W., Liu, J., Fan, X., Carmon, T., Bahl, G. Fabrication and Testing of Microfluidic Optomechanical Oscillators. *J. Vis. Exp.* (87), e51497, doi:10.3791/51497 (2014).

Abstract

Cavity optomechanics experiments that parametrically couple the phonon modes and photon modes have been investigated in various optical systems including microresonators. However, because of the increased acoustic radiative losses during direct liquid immersion of optomechanical devices, almost all published optomechanical experiments have been performed in solid phase. This paper discusses a recently introduced hollow microfluidic optomechanical resonator. Detailed methodology is provided to fabricate these ultra-high-Q microfluidic resonators, perform optomechanical testing, and measure radiation pressure-driven breathing mode and SBS-driven whispering gallery mode parametric vibrations. By confining liquids inside the capillary resonator, high mechanical- and optical- quality factors are simultaneously maintained.

Video Link

The video component of this article can be found at <https://www.jove.com/video/51497/>

Introduction

Cavity optomechanics studies the parametric coupling between phonon modes and photon modes in microresonators by means of radiation pressure (RP)¹⁻³ and stimulated Brillouin scattering (SBS)⁴⁻⁶. SBS and RP mechanisms have been demonstrated in many different optical systems, such as fibers⁷, microspheres^{4,6,8}, toroids^{1,9}, and crystalline resonators^{5,10}. Through this photon-phonon coupling, both cooling¹¹ and excitation^{6,10} of mechanical modes have been demonstrated. However, almost all reported optomechanics experiments are with solid phases of matter. This is because direct liquid immersion of the optomechanical devices results in greatly increased radiative acoustic loss because of the higher impedance of liquids compared against air. In addition, in some situations dissipative loss mechanisms in liquids may exceed the radiative acoustic losses.

Recently, a new type of hollow optomechanical oscillator with a microcapillary geometry was introduced¹²⁻¹⁵, and which by design is equipped for microfluidic experiments. The diameter of this capillary is modulated along its length to form multiple 'bottle resonators' that simultaneously confine optical whispering-gallery resonances¹⁶ as well as mechanical resonant modes¹⁷. Multiple families of mechanical resonant modes participate, including breathing modes, wine-glass modes, and whispering-gallery acoustic modes. The wine-glass (standing-wave) and whispering-gallery acoustic (traveling-wave) resonances are formed when a vibration with integer multiple of acoustic wavelengths occurs around the device circumference. Light is evanescently coupled into the optical whispering-gallery modes of these 'bottles' by means of a tapered optical fiber¹⁸. Confinement of the liquid inside^{19,20} the capillary resonator, as opposed to outside it, enables high mechanical- and optical- quality factors simultaneously, which allows the optical excitation of mechanical modes by means of both RP and SBS. As has been shown, these mechanical excitations are able to penetrate into the fluid within the device^{12,13}, forming a shared solid-liquid resonant mode, thus enabling an opto-mechanical interface to the fluidic environment within.

In this paper we describe fabrication, RP and SBS actuation, and representative measurement results for this novel optomechanical system. Specific material and tool lists are also provided.

Protocol

1. Fabrication of Ultra-high-Q Microfluidic Resonators

1. Preparation of capillary manufacturing setup

1. Fabricate the microfluidic optomechanical resonator in the following way – Heat a glass capillary preform with approximately 10 W of CO₂ laser radiation at 10.6 microns wavelength, and draw out the heated capillary linearly using motorized translation stages. **Figure 1** shows the arrangement of the linear translation stages, the lasers, and the location of the capillary preform before the pulling process.
 2. Program suitable automation software to simultaneously control the two CO₂ lasers (for heating) and the two linear stages. The two linear stages perform the drawing process for the laser-heated capillary.
 3. One of the linear stages must be fast (e.g. 5 mm/sec) for the linear drawing process. Feed in more material to the heating zone with the second, slower linear stage (e.g. 0.5 mm/sec) since the capillary preform material gets depleted during the pulling process.
 4. Align the sample holders on the linear stages along both vertical and horizontal axes.
 5. Carefully align both CO₂ laser beams such that they target the same spot in space (between the sample holders). A piece of card paper or heat sensitive paper is useful for this process. Do not forget to use eye protection for laser safety. Do not lower eyes to table level. Use suitable beam blocks, fume exhaust, and fire protection.
 6. Select reasonable parameters for the drawing process. For example, the following parameters reliably produce a good capillary size — 10 mm/sec pulling speed, 0.5 mm/sec feed-in speed, 3 sec preheating time, 4.5 W preheating powers for both lasers, and 5 W heating powers for both lasers.
 7. Modulation of the laser power during pulling can be used to control the capillary radius lengthwise during the drawing process to form the ‘bottle’ resonators. An example is shown in **Figure 2d**. Select the proper modulation parameters: 3 Hz frequency, 6 W and 3 W for laser powers, and 50% duty cycle.
2. Fabrication of microfluidic optomechanical resonators
 1. Cut a sufficiently long segment (about 2–4 cm) of fused silica capillary such that it can reach the two holders attached to the linear translation stages.
 2. Mount the capillary sample on the sample holders such that the laser target zone is roughly in the middle of the capillary. Readjust CO₂ laser alignment if needed.
 3. Pull the capillary using the parameters as stated in 1.1.6. First preheat the capillary for a few seconds (**Figure 2a**), and then pull it with or without laser modulation (parameters in 1.1.7) as needed.
 4. Remove the drawn capillary (**Figure 2b**) from the sample holder. Handle the sample with gloves at the two thick ends only, in order not to contaminate the clean resonator surface.
 5. Vary the pulling parameters to fabricate capillaries with different diameters. Typically outer diameter varies from 30 µm to 200 µm depending on pulling conditions.
 3. Mounting the fabricated device for testing
 1. Prepare an E shape glass holder (**Figure 2c**). Cut three 1 cm x 0.5 cm and one 3 cm x 0.5 cm glass pieces from glass slides. Assemble them into an E shape using glass adhesive or superglue.
 2. Cut a length of microfluidic capillary out of the drawn sample. This length should be longer than the distance between two adjacent glass branches on the E shape holder.
 3. Glue the microcapillary device onto the holder using optical adhesive while making sure to keep a portion hanging uncontaminated between two branches of the E shape holder. Cure the optical adhesive with a LED UV curing light source for 10 sec. **Figures 2c** and **2d** show the finished product.
 4. Carefully insert both ends of the mounted resonator into two slightly larger plastic tubes (e.g. 200 µm in inner diameter). Glue and UV cure both ends to the plastic tubes with optical adhesive.
 5. Clamp the E shape structure from the third (free) glass branch to a clamped mounting device for testing. The optical quality factor of the final microfluidic resonator depends on how well the fabrication lasers were aligned and how stable their power levels were.

2. Experimental Setup for Optomechanical Testing

1. Fabrication of tapered optical fiber
 1. Prepare a single mode telecom-band optical fiber of desired length (e.g. a few feet). Fiber segment should be long enough to be both mounted in the tapering area and connected to the setup (**Figure 4**). The tapering method explained here is similar to what is suggested and demonstrated in ²².
 2. Connect the prepared fiber segment to the rest of the experimental setup using any convenient fiber-splicing method.
 3. Mount the spliced fiber segment onto two linear pullers that face each other.
 4. Strip off the fiber jacket in the center of the mounted fiber fragment to expose cladding area. This is where taper will be fabricated. Clean the stripped area with methanol.
 5. Turn on the tunable laser to see real-time transmission on an oscilloscope. Make sure to set attenuators so that photodetectors are not damaged.
 6. Place a narrow nozzle hydrogen gas burner immediately underneath the unjacketed portion of the fiber. Follow all recommended safety procedures when working with pressurized flammable gases such as hydrogen. Other “clean burning” sources of flame or ceramic heaters could also be used.
 7. Before lighting up the gas, check the flow rate so that flame will not be too large (a 1–2 cm tall flame is adequate). Note that the flame is mostly invisible but may be seen as a faint orange glow in a dark room. The hydrogen flow rate should be set to a point where lighted flame will adequately soften the glass fiber.
 8. Light up the flame. As soon as flame is on, start pulling the fiber using motorized stages. Appropriate pulling speed depends on flow rate of hydrogen gas and vicinity of the flame. NOTE: Transmission through the fiber will begin to show temporal oscillation behavior as pulling continues. This indicates multimode operation.
 9. When oscillatory behavior stops and shows an unchanging signal over time, stop pulling and turn-off the flame immediately. This is when single-mode taper is obtained. Check the transmission. If transmission is too low, repeat the procedure from 2.1.1. with modified gas flow rate, flame size, and flame location. On occasion, low transmission could be due to bad alignment at step 2.1.3. or due to contamination of the exposed cladding.

10. If resultant transmission through the taper is satisfactory, wait a few minutes to cool down the taper.
 11. Inspect the taper under a microscope. For 1,550 nm operational wavelength, typical diameter of the single-mode taper is in the order of 1-2 μm .
2. Taper-coupling to WGR and searching for electronic signals indicating vibration
 1. Set up the experiment in the configuration shown in **Figure 3**. Mechanical vibrations can be generated through both SBS and RP by the same experimental configuration. In order to clearly detect back-scattered signals as in the case of backward-SBS^{4,21}, use a circulator between taper and tunable laser.
 2. Before turning on the tunable IR laser, make sure to set attenuators in place so that photodetectors are not damaged.
 3. Turn on and stabilize the tunable IR laser. A function generator is used to sweep the frequency of the input IR laser.
 4. Mount the resonator holder on a nanopositioning stage. Carefully bring the resonator close to the tapered fiber in order to obtain evanescent coupling. As the laser frequency is swept, optical resonances will appear as dips in transmission in the oscilloscope, as in **Figure 2b** of²².
 5. Connect the photodetector output to an electrical spectrum analyzer (ESA), where the temporal interference (*i.e.* beat note) between the input laser light and the scattered light can be observed. This temporal interference occurs at the mechanical oscillation frequency. The "peak hold" function on the spectrum analyzer is often useful in the initial search for mechanical vibrations.
 6. Use higher input power while performing the initial search for mechanical vibration, especially when liquids are present inside the device. NOTE: Typically, input power in the order of 100 μW to the device is sufficient to excite mechanical vibration.
 7. If mechanical oscillation is observed, attempt to lock to the relevant optical mode by turning off the laser frequency scan and controlling the laser wavelength in CW mode. Here, both oscilloscope and spectrum analyzer are useful in tandem. Periodic signals appear on the oscilloscope when a mechanical mode is present, as seen in **Figure 5** and^{1,6}.

3. Measuring Optomechanical Vibrations

1. Optical and electronic signature of radiation pressure (RP) modes
 1. As described in 2.2, mechanical oscillations will be observed when the taper and device are correctly coupled, the device optical and mechanical modes have sufficient Q-factors, and sufficient input optical power is provided. If oscillations in the range of 10 MHz - 1 GHz are not observed, attempt to change polarization to investigate different resonances, or increase the input power from tunable laser in order to overcome the minimum threshold for oscillation. When increasing the input power, always be careful not to saturate the photodetectors. Also, as described in⁸, coupling distance is a key factor for exciting different RP modes.
 2. If mechanical modes are still not observed, try measuring optical quality factor. For microfluidic optomechanical resonators, results show that optical quality factor of 10^6 is sufficient to excite parametric oscillations¹³. NOTE: Usually, RP modes will manifest as electronic oscillations on the spectrum analyzer accompanied by their harmonics, as seen in **Figure 5**. Representative results will be discussed in section 4.
 3. Use a scanning Fabry-Perot interferometer or high-resolution optical spectrum analyzer to detect the optical side bands that are generated due to amplitude and phase modulation, which is in turn induced by the periodic cavity deformation. An example measurement may be seen in **Figure 3h** of¹.
2. Optical and electronic signature of whispering-gallery acoustic modes
 1. The acoustic frequency of backward-SBS for silica glass is approximately 11 GHz when a 1.5 micron pump laser is used^{4,23}. Use a circulator that monitors the back-scattered light and some small amount of Rayleigh-scattered pump, to observe electronic signals for these vibrational modes. Use a high-resolution optical spectrum analyzer to resolve the scattered light. An example measurement is shown in **Figure 2** of⁴.
 2. Use the beat note between forward scattered light and the pump laser to observe lower frequency (sub-1 GHz) whispering-gallery acoustic modes.
 3. Due to the lower mechanical rigidity in the breathing direction, the signal from SBS is sometimes weaker than the signal from the RP modes. Again, sweep the laser at slow speed, and use "peak hold" on the spectrum analyzer to help in finding the SBS signal.
 4. Note that unlike RP-excited breathing modes, SBS-excited whispering-gallery acoustic modes do not exhibit harmonics in the optical and electronic spectra (unless cascaded excitation takes place^{4,24}). Instead only one Stokes sideband appears for SBS modes.

Representative Results

The capillaries produced by this method are thin (between 30 μm and 200 μm), clear, and very flexible, but are sufficiently robust for direct handling. It is important to protect the outer surface of the capillary device against dust and water (moisture) in order to maintain a high optical quality factor (Q). By dipping one end of the capillary in water and blowing air through the capillary by means of a syringe, it can be verified whether the capillary is through or whether was sealed off during fabrication due to overheating.

A tunable laser can be used to probe the optical modes of the fabricated device by means of tapered fiber waveguide coupling. In this test, sharp optical resonances are expected indicating high optical Q-factor. An additional indication for high Q-factor is the thermal broadening of the optical modes²⁵.

When RP-actuated parametric oscillation takes place, harmonics of the mechanical mode will be seen in the optical spectrum obtained on the output port of the tapered waveguide. This occurs due to the large modulation depth of the amplitude and phase modulation of the light, caused by the mechanical vibrations. Examples of the typically observed electrical spectrum are seen in **Figure 5a** and also in¹. An oscilloscope trace of the signal exhibits periodic behavior (**Figure 5b**). Finite element analysis can be invoked to model the mechanical modes of the system, to confirm that the observed optical modulation corresponds to an eigenmechanical frequency. SBS driven mechanical modes are easily identified

by the absence of harmonics of the fundamental mechanical signal, since only a single Stokes sideband is generated⁶. These modes typically occur at higher frequencies than the RP modes, although low frequencies are possible as well.

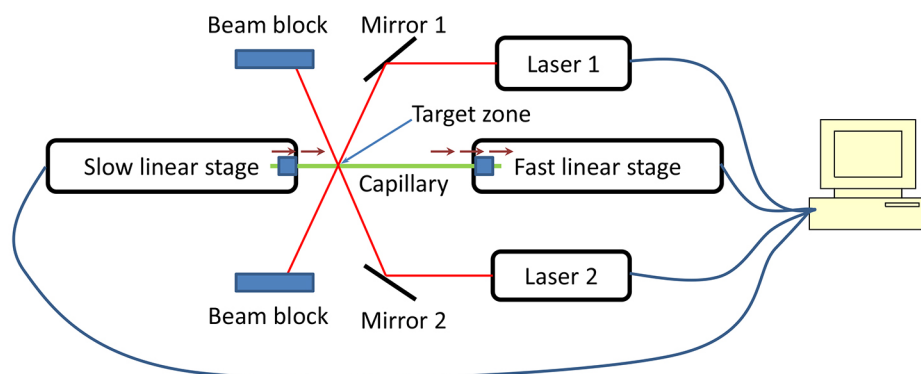


Figure 1. Schematic of the capillary pulling setup. The microfluidic optomechanical resonators are drawn from a larger capillary preform attached to two linear stages while the glass is heated by the CO₂ laser. Both laser beams are carefully aligned to the same spot of the capillary. Moving direction and relative speeds of the linear stages are indicated by the arrows. [Please click here to view a larger version of this figure.](#)

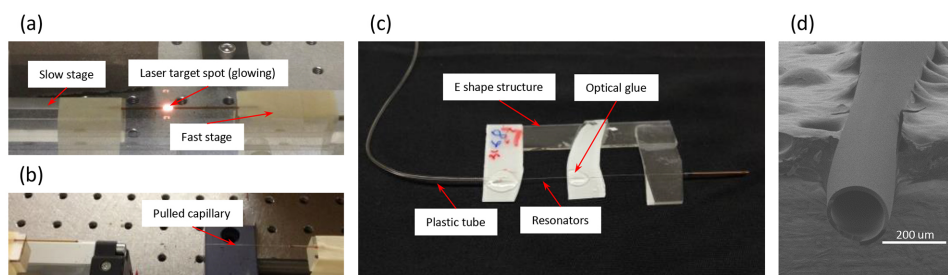


Figure 2. Optomechanical bottle resonator fabrication. (a) The capillary preform is pulled at a constant speed while being heated by means of CO₂ laser radiation. Note the glowing region is the laser target spot (where the beams heat the silica). When the required length and diameter are reached, (b) stop the linear stage motion and turn the lasers off. The pulled capillary is thin, clear, and very flexible. (c) Employ an E shape glass structure to mount the microcapillary resonator device as described in section 1.3. The optomechanical bottle resonator is now ready to be taken to the experimental setup and connected to tubing that will provide analytes. (d) Scanning electron micrograph of the fabricated optomechanical bottle resonator. Resonator radius and wall thickness can be varied as needed. [Please click here to view a larger version of this figure.](#)

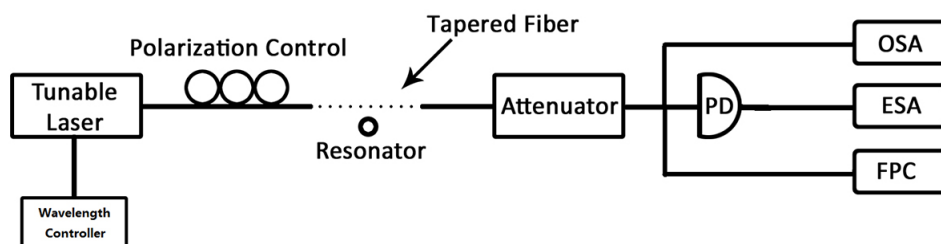


Figure 3. Schematic of the testing setup. Light is evanescently coupled into the resonator through a tapered fiber. A tunable IR laser (1,520–1,570 nm) is used as the light source and is fine-tuned to match a chosen optical mode of the resonator. Mechanical vibrations actuated by light in the resonator cause modulation of the input light at the mechanical vibration frequency. The electric fields of the optical pump and vibration-scattered light in the forward direction interfere temporally on the photodetector (PD) at the end of the tapered fiber. A beat note between the two optical signals is thus generated through the optical-power-to-current transduction taking place in the photodetector. This beating can be observed on an electric spectrum analyzer (ESA). A scanning Fabry-Perot cavity (FPC) and optical spectrum analyzer (OSA) can also be used to directly observe the optical side bands that are generated due to the modulation. [Please click here to view a larger version of this figure.](#)

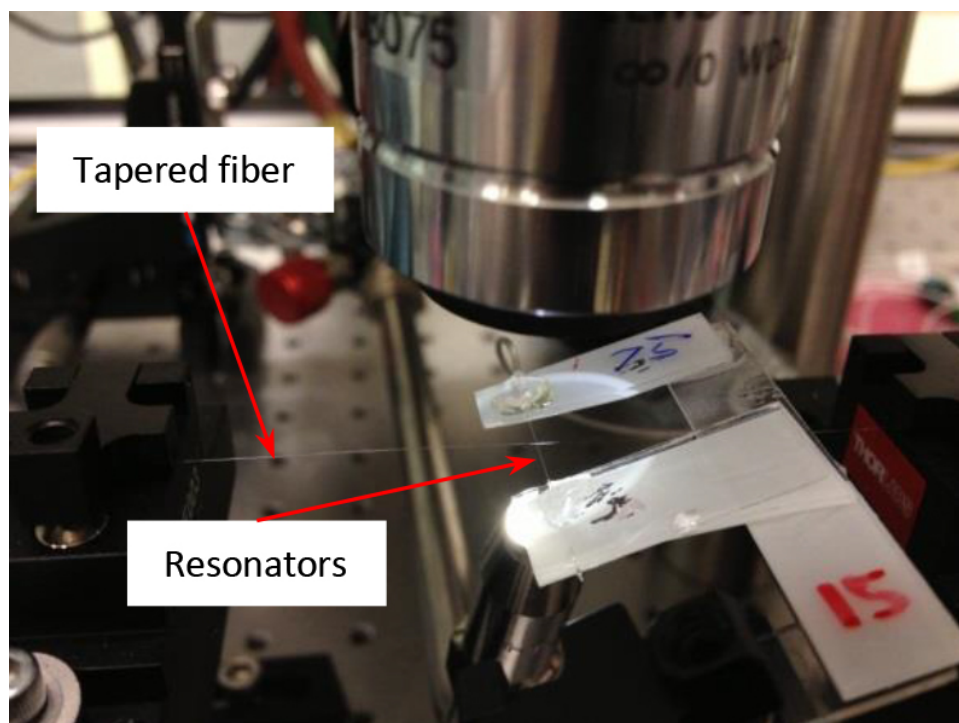


Figure 4. Coupling light from a fiber to micro resonator. The E shape structure is mounted just above the tapered fiber so that light can be evanescently coupled into the resonators. [Please click here to view a larger version of this figure.](#)

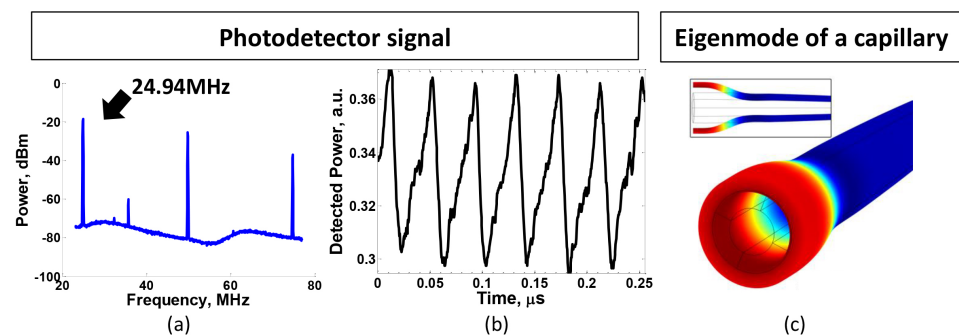


Figure 5. Representative results. (a) A breathing mechanical mode at 24.94 MHz in the microcapillary is excited by centrifugal radiation pressure by light circulating in an optical mode. Modulation of the input light by this mechanical vibration is observable on an electrical spectrum analyzer through beat-note generation on a photodetector placed in the forward-scattering direction (See **Figure 3**). (b) An oscilloscope trace of the photodetector output signal (*i.e.* transmitted power) shows the periodic temporal interference of the input light and scattered light. (c) Finite element simulation for the corresponding breathing mode confirms that the observed optical modulation corresponds to an eigenmechanical frequency. Colors represent deformation and the simulation is sliced at the capillary mid-point for presentation. [Please click here to view a larger version of this figure.](#)

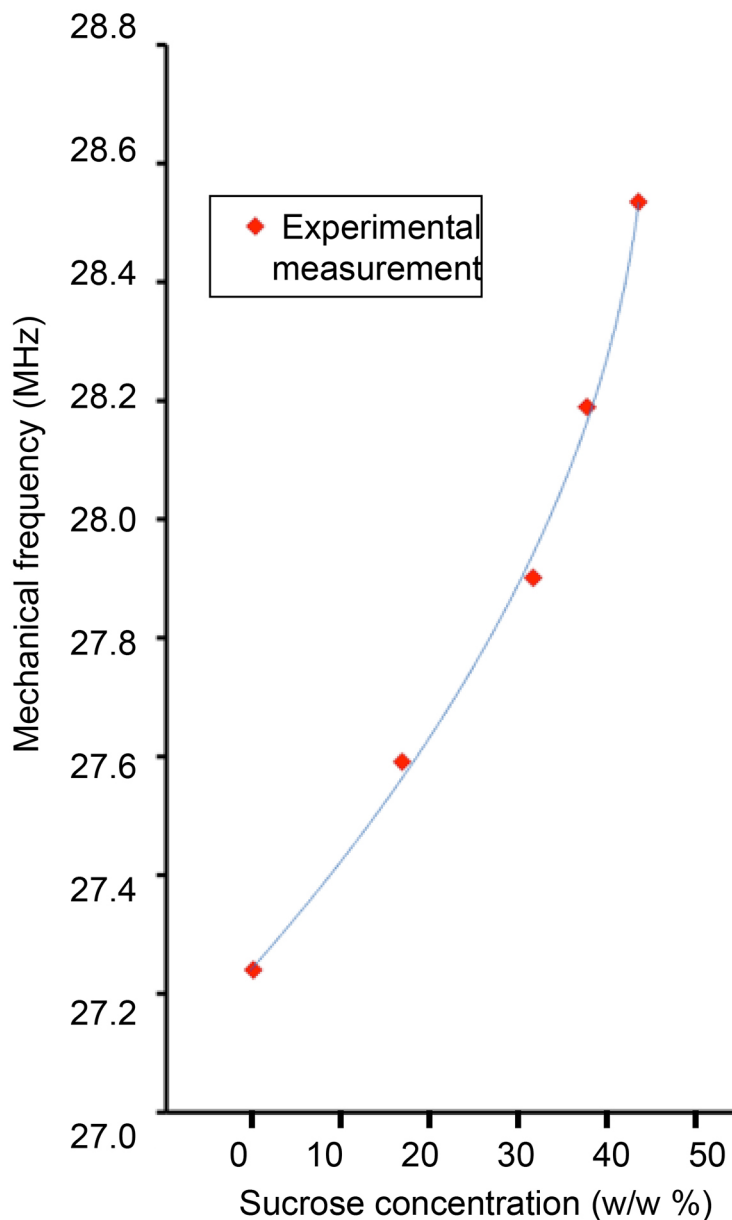


Figure 6. The mechanical frequency is presented as a function of the fluid density. The same mechanical mode is measured on the same device with different concentrations of sucrose solutions present inside. [Please click here to view a larger version of this figure.](#)

Discussion

We have fabricated and tested a new device that bridges between cavity optomechanics and microfluidics by employing high-Q optical resonances to excite (and interrogate) mechanical vibration. It is surprising that multiple excitation mechanisms are available in the very same device, which generate a variety of mechanical vibrational modes at rates spanning 2 MHz to 11,300 MHz. Centrifugal radiation pressure supports both wineglass modes and breathing modes in the 2-200 MHz span, Forward stimulated Brillouin scattering allows mechanical whispering gallery modes in the 50-1,500 MHz range, and lastly, backward stimulated Brillouin scattering excites mechanical whispering gallery modes near 11,000 MHz.

The methods that are described in the current work enable the fabrication of these microfluidic resonators with ultra-high optical quality factors of about 10^8 . Simultaneously, since liquids are now confined within the device, acoustic losses are brought under control and the device is able to maintain a high mechanical quality factor as well. With this platform, we have demonstrated that the density changes of a fluid contained within the device can be measured (**Figure 6**). In order to fully understand the opto-mechano-fluidic coupling that enables this, future work will involve multiphysical modeling of the device.

There are a few practical challenges associated with this fabrication method. For instance, the capillary material must be a good absorber for the 10.6 micron CO_2 laser radiation so that it can heat up sufficiently for the pulling process to take place. In this regard, the materials that have been

tested for capillary fabrication are silica and quartz. Furthermore, the circular symmetry of the capillary is dictated by the relative power balance between the two lasers that are employed during the pulling step, and by the location of the capillary in the laser target zone. Since the circular symmetry of the device is a key parameter for maintaining high optical and mechanical quality factor, misalignment of the capillary preform in the CO₂ laser target zone before pulling or during pulling can be a concern and care must be taken to keep this under control.

On the other hand, this fabrication method provides a lot of flexibility in the fabrication of silica-based optomechanical capillary resonators. By modulating the CO₂ laser power, the capillary diameter can be varied quite easily to suit the application. On demand spacing between adjacent bottle resonators is possible thanks to the high degree of computer control. Finally, control of the rate of pulling and the rate of “feed in” of the capillary preform provides an easy knob for controlling the capillary diameter.

In conclusion, the silica-based microcapillary platform as described is a low-cost, high-performance optical and optomechanical system that can be applied to a variety of studies with non-solid phase materials, including superfluids, and bio-analytes such as living cells. These devices can additionally leverage the very large body of literature on surface acoustic wave sensing of gases and liquids. As a result, this is an enabling technology for optical sensing applications.

Disclosures

We have nothing to disclose.

Acknowledgements

This work was funded by Startup funding from the University of Illinois at Urbana-Champaign, DARPA ORCHID program through a grant from AFOSR, the National Science Foundation through grant CMMI-1265164, and the National Science Foundation Graduate Research Fellowship program. We acknowledge enlightening discussions with Prof. Jack Harris, Prof. Pierre Meystre, Dr. Matt Eichenfield, Prof. Taher Saif, and Prof. Rashid Bashir.

References

- Carmon, T., Rokhsari, H., Yang, L., Kippenberg, T., Vahala, K. Temporal Behavior of Radiation-Pressure-Induced Vibrations of an Optical Microcavity Phonon Mode. *Physical Review Letters*. **94** (22). doi:10.1103/PhysRevLett.94.223902, (2005).
- Rokhsari, H., Kippenberg, T., Carmon, T., Vahala, K. J. Radiation-pressure-driven micro-mechanical oscillator. *Optics Express*. **13** (14), 5293–5301. doi:10.1364/OPEX.13.005293, (2005).
- Kippenberg, T. J., Rokhsari, H., Carmon, T., Scherer, A., Vahala, K. J. Analysis of Radiation-Pressure Induced Mechanical Oscillation of an Optical Microcavity. *Physical Review Letters*. **95** (3), 033901. doi:10.1103/PhysRevLett.95.033901, (2005).
- Tomes, M., Carmon, T. Photonic Micro-Electromechanical Systems Vibrating at X-band (11-GHz) Rates. *Physical Review Letters*. **102**(11), 113601. doi:10.1103/PhysRevLett.102.113601, (2009).
- Grudinin, I. S., Matsko, A. B., Maleki, L. Brillouin lasing with a CaF₂ whispering gallery mode resonator. *Physical Review Letters*. **102** (4), 043902, (2009).
- Bahl, G., Zehnpfennig, J., Tomes, M., Carmon, T. Stimulated optomechanical excitation of surface acoustic waves in a microdevice. *Nature Communications*. **2** (403). doi:10.1038/ncomms1412, (2011).
- Dainese, P., Russell, et. al. A. Stimulated Brillouin scattering from multi-GHz-guided acoustic phonons in nanostructured photonic crystal fibres. *Nature Physics*. **2** (6), 388–392. doi:10.1038/nphys315, (2006).
- Carmon, T., Cross, M. C., Vahala, K. J. Chaotic Quivering of Micron-Scaled On-Chip Resonators Excited by Centrifugal Optical Pressure. *Physical Review Letters*. **98** (16), 167203. doi:10.1103/PhysRevLett.98.167203, (2007).
- Armani, D., Min, B., Martin, A., Vahala, K. J. Electrical thermo-optic tuning of ultrahigh-Q microtoroid resonators. *Applied Physics Letters*. **85** (22), 5439–5441. doi:10.1063/1.1825069, (2004).
- Savchenkov, A. A., Matsko, A. B., Ilchenko, V. S., Seidel, D., Maleki, L. Surface acoustic wave opto-mechanical oscillator and frequency comb generator. *Optics Letters*. **36** (17), 3338–3340. doi:10.1364/OL.36.003338, (2011).
- Bahl, G., Tomes, M., Marquardt, F., Carmon, T. Observation of spontaneous Brillouin cooling. *Nature Physics*. **8** (3), 203–207. doi:10.1038/nphys2206, (2012).
- Bahl, G., Kim, K. H., Lee, W., Liu, J., Fan, X., Carmon, T. Brillouin cavity optomechanics with microfluidic devices. *Nature Communications*. **4** (1994), doi:10.1038/ncomms2994, (2013).
- Kim, K. H., et al. Cavity optomechanics on a microfluidic resonator with water and viscous liquids, accepted for publication in *Light: Science and Applications*. available: <http://arxiv.org/abs/1205.5477>, (2013).
- Sumetsky, M., Dulashko, Y., & Windeler, R. S. Optical microbubble resonator. *Optics Letters*. **35** (7), 898–900. doi:10.1364/OL.35.000898, (2010).
- Lee, W., et al. A quasi-droplet optofluidic ring resonator laser using a micro-bubble. *Applied Physics Letters*. **99** (9), 091102–091102–3. doi:10.1063/1.3629814, (2011).
- Junge, C., Nickel, S., O’Shea, D., Rauschenbeutel, A. Bottle microresonator with actively stabilized evanescent coupling. *Optics Letters*. **36** (17), 3488–3490. doi:10.1364/OL.36.003488, (2011).
- Bahl, G., Fan, X., Carmon, T. Acoustic whispering-gallery modes in optomechanical shells. *New Journal of Physics*. **14** (11), 115026. doi:10.1088/1367-2630/14/11/115026, (2012).
- Cai, M., Painter, O., Vahala, K. Observation of Critical Coupling in a Fiber Taper to a Silica-Microsphere Whispering-Gallery Mode System. *Physical Review Letters*. **85** (1), 74–77. doi:10.1103/PhysRevLett.85.74, (2000).
- Burg, T. P., Manalis, S. R. Suspended microchannel resonators for biomolecular detection. *Applied Physics Letters*. **83** (13), 2698. doi:10.1063/1.1611625, (2003).

20. Burg, T. P., *et al.* Weighing of biomolecules, single cells and single nanoparticles in fluid. *Nature*. 446(7139), 1066–9. doi:10.1038/nature05741, (2007).
21. Li, J., Lee, H., Chen, T., Vahala, K. J. Characterization of a high coherence, Brillouin microcavity laser on silicon. *Optics Express*. **20** (18), 20170. doi:10.1364/OE.20.020170, (2012).
22. Knight, J. C., Cheung, G., Jacques, F., Birks, T. A. Phase-matched excitation of whispering-gallery-mode resonances by a fiber taper. *Opt. Lett.* **22** (15): 1129-1131, DOI: 10.1364/OL.22.001129, (1997).
23. Boyd, R. W. *Nonlinear Optics*. Acad. Press. (2003).
24. Li, J., Lee, H., Vahala, K. J. Microwave synthesizer using an on-chip Brillouin oscillator. *Nature Communications*. **4** (2097). doi:10.1038/ncomms3097, (2013).
25. Carmon, T., Yang, L., Vahala, K. Dynamical thermal behavior and thermal self-stability of microcavities. *Optics Express*. **12** (20), 4742–4750. doi:10.1364/OPEX.12.004742, (2004).